

Supplemental material for

Adenosine A₃ agonists reverse neuropathic pain via T cell-mediated production of IL-10

Mariaconcetta Durante^{1,2,a}, Silvia Squillace^{1,3,4,a}, Filomena Lauro^{1,3,5,a}, Luigino Antonio Giancotti^{1,3}, Elisabetta Coppi², Federica Cherchi², Lorenzo Di Cesare Mannelli², Carla Ghelardini², Grant Kolar^{3,6}, Carrie Wahlman¹, Adeleye Opejin⁷, Cuiying Xiao⁸, Marc L. Reitman⁸, Dilip K. Tosh⁸, Daniel Hawiger⁷, Kenneth A. Jacobson⁸ and Daniela Salvemini^{1,3*}

^aCo-first authors

¹Department of Pharmacology and Physiology, Saint Louis University School of Medicine, 1402 South Grand Blvd, St. Louis, MO 63104, USA.

²Department of Neuroscience, Psychology, Drug Research and Child Health (NEUROFARBA), Section of Pharmacology, University of Florence, Viale Gaetano Pieraccini, 6 - 50139 Florence, Italy.

³Henry and Amelia Nasrallah Center for Neuroscience, Saint Louis University School of Medicine, 1402 South Grand Blvd., St. Louis, MO 63104, USA;

⁴Department of Physiology and Pharmacology "V. Erspamer", Sapienza University of Rome, Italy.

⁵Institute of Research for Food Safety & Health (IRC-FSH), Department of Health Sciences, University "Magna Graecia" of Catanzaro, Catanzaro, Italy.

⁶Department of Pathology, Saint Louis University School of Medicine, St. Louis, MO 63104 USA.

⁷Department of Molecular Microbiology and Immunology, Saint Louis University School of Medicine, 1402 South Grand Blvd, St. Louis, MO 63104, USA.

⁸National Institute of Diabetes and Digestive and Kidney Diseases, NIH, Bethesda, Maryland 20892, USA.

*Corresponding author: E-mail address: daniela.salvemini@health.slu.edu. Address: 1402 South Grand Blvd, St. Louis, MO 63104, USA, Phone: 1-314-977-6430, Fax: 1-314-977-6411

Disclosure of Potential Conflicts of Interest: Dr. Salvemini is founder of BioIntervene, Inc., a company developing A₃AR agonists for clinical use. All other authors have declared that no conflict of interest exist.

Supplemental Methods

Animals

Adult male or female mice (20-30 g) *Rag*^{KO}, *Il10*^{KO}, *Il10r*^{KO}, wild-type (WT; C57BL/6) and WT-GFP (green fluorescent protein) mice were purchased from The Jackson Laboratory (Bar Harbor, ME, USA). The A₃AR knockout (*Adora3*^{KO}) mice (1), on a C57BL/6 genetic background, were genotyped by PCR (*Adora3* forward common primer 5'-ACTGGCCCCATACACAACCTG, *Adora3* reverse primer 5'-AGACAATGAAATAGACGGTGGTG, and *Neo* reverse primer 5'-ATGGAAGGATTGGAGCTACG), producing 208 bp WT and ~400 bp null allele products). Mice were housed 5/cage in a controlled environment (12-h light-dark cycles) with food and water available *ad libitum*. Procedures for the maintenance and use of animals were in accordance with the International Association for the Study of Pain (Seattle, MD) and NIH (Bethesda, MD) guidelines on laboratory animal welfare and approved by the Saint Louis University Animal Care and Use Committee (IACUC), the National Institute of Diabetes and Digestive and Kidney Diseases IACUC, and by the animal Ethical and Care Committee of the University of Florence (Florence, Italy). All experiments were conducted with the experimenters blinded to treatment conditions. No signs of colitis were observed in *Il10*^{KO} mice.

Reagent preparation and administration

Test compound include MRS5980, (1*S*,2*R*,3*S*,4*R*,5*S*)-4-(2-((5-chlorothiophen-2-yl)ethynyl)-6-(methylamino)-9H-purin-9-yl)-2,3-dihydroxy-N-methylbicyclo[3.1.0]hexane-1-carboxamide, synthesized as previously described (2, 3), and morphine sulfate was purchased from Millipore-Sigma (St. Louis, MO, USA). Phosphate buffered saline (PBS) 1X, pH 7.4, was used as vehicle.

The highly selective A₃AR agonists, MRS5980 (1 mg/kg) (5), were administered intraperitoneally (i.p.) on day 8 (D8) after CCI surgery.

Estrus smears

Mice vaginal smears were taken daily for 7 days before and after the experiment to verify normal cyclicity. Cells were placed on a glass slide and analyzed with a light microscope to determine their stage of estrus cycle as described (6). All animals displayed a normal 4- to 5-day estrus cycle.

CCI model of neuropathic pain

Chronic constriction injury of the sciatic nerve was done as previously described (7). Briefly, mice (weighing 25–30 g at the time of surgery) were anesthetized with 3% isoflurane/100% O₂ inhalation and maintained on 2% isoflurane/100% O₂ for the duration of surgery. The left thigh was shaved and scrubbed with Nolvasan, and a small incision (1–1.5 cm in length) was made in the middle of the lateral aspect of the thigh to expose

the sciatic nerve. The nerve was loosely ligated at 2 sites spaced 1 mm apart using 6.0 silk suture. The surgical site was closed with a skin clip.

Behavioural testing

Mechanical allodynia was assessed as the hind paw withdrawal response to von Frey hair stimulation using the up-and-down method (8), as previously described (9). Briefly, the animals were first acclimatized (30 min) in individual clear Plexiglas boxes on an elevated wire mesh platform to facilitate access to the plantar surface of the hind paws. Subsequently, a series of von Frey hairs (0.04, 0.07, 0.16, 0.4, 0.6, 1.0, 1.4 and 2 g; Stoelting, Wood Dale, IL USA) were applied perpendicular to the hind paw plantar surface, until the filament buckled and then held for 2–5 s. A test began with the application of the 0.6-g hair. A positive response was defined as clear paw withdrawal or paw shaking. In the event of a positive response, the next lighter hair was applied; whereas the next heavier hair was applied in the event of a negative response. At least four readings are obtained after the first positive response and the pattern of response was converted to a 50% paw withdrawal threshold (PWT), using the method described by Chaplan (10) before statistical analysis. Mechano-allodynia was defined as a significant (2 SD) decrease in the measured behavior compared to the individual animal's baseline behavior prior to mechanical or pharmacological pain induction.

At the end of behavioral testing, CCI mice were deeply anesthetized (ketamine 110 mg/kg/xylazine 11 mg/kg - 0.1 ml/10g of body weight), perfused with ice cold PBS 1X and DRGs were isolated from the lumbar enlargement (L4-L6) region of the spinal cord as previously described (11) for immunofluorescence and Western blot analysis.

T cells isolation and adoptive transfer

Single-cell suspensions were obtained from spleens and lymph nodes of C57BL/6 WT, WT-GFP, *Il10*^{KO}, *Il10r*^{KO}, and *Adora3*^{KO} mice by passing the tissue through 70µm strainers, after which cells were washed with PBS plus 0.1% bovine serum albumin. T-cell population was purified by negative selection. Briefly, T-cells were incubated with biotinylated antibodies against CD11b (#101204), CD11c (#117304), CD49b (#108904), B220 (#103204), TER-119(#116204), CD4 (#100404) or CD8a (#100704), all purchased from BioLegend, and they were negatively selected by autoMACS sorting. Flow cytometry analysis showed purity of isolated cells > than 95% (**Fig. S9**). After MACS purification, T-cells were washed, counted and resuspended in PBS for intravenous injections (2 x 10⁶/200µl/mouse). On Day 7 after CCI surgery, T cells or PBS 1X were injected intravenously (i.v.) into the tail vein in a volume of 200µl. An aliquot of the sorted population was assessed for the purity: cells were labeled with anti-CD3-FITC (#100305), anti-CD8-PerCpCy5 (#100733) or with anti-CD4-PeCy7 (#100421; Biolegend, San Diego, CA) and purity was confirmed by flow cytometry.

Immunofluorescence

DRGs were incubated with NucBlue diluted in 1X PBS pH 7.4 at manufacturer recommended concentration (2 drops per 1 ml) (ThermoFisher) for 15 minutes to stain nuclei. Samples were washed 2x in 1X PBS pH 7.4 and briefly dried by touching a paper towel and placed between a slide and coverslip. Moderate pressure was applied to the coverslip to flatten and spread the specimen. Axial stacks of entire DRGs were imaged at 40x (NA 0.95) for DAPI and GFP on an epifluorescent Leica DM6 fitted with an automated Z stage (Leica Microsystems, Exton, PA) and CoolLED pE-300 white illumination system (Andover, NY) and 460/50, 527/30 excitation filters. DAPI signal was subtracted from GFP in FIJI (12) followed by manual cell counting. For Figure 3D, a mean z projection was generated using the CLIJ plugin (13) in ImageJ (FIJI), cropped and zoomed to equivalent areas for the DAPI and GFP channels.

Western Blot analysis

Harvested DRGs were immediately stored at -80°C . Briefly, frozen tissues were homogenized in lysis buffer [20 mM Tris-Cl, pH 7.4, 150 mM NaCl, 1% Triton X-100, 1 mM EDTA, 0.1% SDS, 2.5% glycerol, 50 mM sodium fluoride, 1 mM sodium orthovanadate, 1 mM sodium molybdate, 1 mM PMSF, 1x phosphatase inhibitor mixture (Sigma-Aldrich), and 1x protease inhibitor mixture (Sigma-Aldrich)], sonicated, and clarified by centrifugation. Total protein concentration was determined by BCA, and samples were heat denatured in 2x Laemmli buffer supplemented with β -mercaptoethanol. Proteins were resolved by Tris-glycine-SDS electrophoresis with a 7.5% gel and transferred to PVDF membrane (Bio-Rad). After blocking with 5% BSA in TBS-T, the membranes were probed overnight at 4°C with primary antibody for GluN2B-Y1472p (1:100; #AB5403; Millipore Corporation, Temecula, CA, USA). Bands were visualized with secondary HRP-conjugated anti-rabbit IgG antibodies (#7074S; Cell Signaling Technology, 1:10000). Immunoblot images were captured and analyzed using ChemiDoc MP and Image Lab 5.0 (Bio-Rad). All data are expressed as the percentage densitometric signal normalized to respective α -tubulin (#T82023; Sigma, St. Louis, MO, USA) loading control.

RT-qPCR

DRG cell cultures were lysed using TRIzolTM (Sigma-Aldrich, Italy), 500ng of total RNA obtained were retro-transcribed using iScript (Bio-Rad) and amplified using a RotorGene 3000 (Qiagen) Instrument. Primers were purchased from IDT (Germany). PCR amplification was carried out by SsoAdvancedTM Universal SYBR[®] Green Supermix (Bio-Rad) according to manual instruction. In the present analysis 18s rRNA was used as the normalizer. The RT-qPCR was performed using the following procedure: 98°C for 2 min, 40 cycles of 98°C for 5 sec, 60°C for 10 sec. The program was set to reveal the melting curve of each amplicon from 60°C to 95°C with a read every 0.5°C . Primers are as follows: Glial fibrillary acidic protein (GFAP) Fw 5'-

CCCTGGCTCGTGTGGATTGGAG-3' Rv 5'-TGGCCACTGCCTCGTATTGAGTGC-3';
 NeuN Fw 5'- CATCAGCCACAGAAGCTATGGAAACG -3' Rv 5'-
 CACACCGTGGAAGCATACAGAATGGT-3'; 18s Fw 5'-
 CGGCTTGGTGACTCTAGATAACCTCG-3' Rv 5'-
 GCGACTACCATCGAAAGTTGATAGGG-3'.

Co-culture of primary mouse DRG neurons with CD4⁺ or CD8⁺-T

DRG were isolated from C57BL/6 WT mice (7-8 weeks old, Envigo, Varese, Italy) as described (14). Briefly, ganglia were bilaterally excised and enzymatically digested using 2 mg/ml of papain and 1 mg/ml of trypsin in Hank's Balanced Salt Solution (HBSS) for 35 min at 37 °C. Cells were resuspended in Dulbecco's Modified Eagle's Medium (DMEM) supplemented with 10% heat inactivated horse serum, 10% heat-inactivated fetal bovine serum (FBS), 100 U/ml penicillin, 0.1 mg/ml streptomycin and 2 mM L-glutamine for mechanical digestion. After centrifugation (1,200 g for 5 min), cells were re-suspended in the same medium and plated on 13 mm glass coverslips coated by poly-L-lysine (8.3 mM) and laminin (5 mM) for 1–2 days before being used for electrophysiological experiments. Cultures obtained by this procedure contained 95% NeuN⁺ and 5% GFAP⁺ cells (n=5; **Fig. S10**). DRG neurons were co-cultured with primary CD4⁺ or CD8⁺-T isolated from C57BL/6 WT mice, as previously described. In some experiments, co-cultures were prepared by isolating DRG neurons, CD4⁺ or CD8⁺-T from CCI C57BL/6 mice 7 days after nerve ligation. In this case, only lumbar DRG (L4-L6) ipsilateral to injury were isolated. Co-cultures of CD4⁺ or CD8⁺-T (10⁵ cells/well) and DRG neurons (10⁴ cells/well) were incubated overnight at 37°C and the following day used for electrophysiology analysis.

Electrophysiology

Whole-cell patch-clamp recordings were performed on small-medium sized (Cm < 25 pF) DRG neurons, as described (14). Extracellular solution (in mM): NaCl 147; KCl 4; MgCl₂ 1; CaCl₂ 2; HEPES (4-(2-hydroxyethyl)-1-piperazineethanesulfonic acid) 10; D-glucose 10 (pH 7.4 with NaOH). Pipette solution (in mM): K-gluconate 130; NaCl 4.8; KCl 10; MgCl₂ 2; CaCl₂ 1; Na₂-ATP 2; Na₂-GTP 0.3; EGTA 3; HEPES 10 (pH 7.4 with KOH). All voltage values have been corrected for the liquid junction potential which was calculated to be 14.1 mV. Cells were transferred to a 1 ml recording chamber (at room temperature) mounted on the platform of an inverted microscope (Olympus CKX41, Milan, Italy) and superfused at a flow rate of 1.5 ml/min by a three-way perfusion valve controller (Harvard Apparatus). Borosilicate glass electrodes (Harvard Apparatus, Holliston, MA) were pulled with a Sutter Instruments puller (model P-87) to a final tip resistance of 2–3 MΩ. Data were acquired with an Axopatch 200B amplifier (Axon Instruments, CA), digitized at 50 kHz and filtered at 10 kHz, stored and analysed with pClamp 9.2 software (Axon Instruments, CA). Cell capacitance (Cm) was measured from the amplifier circuitry and was used to estimate neuronal diameter by assuming an approximated spherical cell

shape accordingly to the calculated C_m for all biological membranes of $1 \mu\text{F}/\text{cm}^2$ (16) and to the sphere surface equation: $A=4\pi r^2$. Current-clamp recordings were performed as described (15). A ramp current protocol consisting in 1 s injection of 30 pA positive current from the resting membrane potential was applied once every 30 sec to evoke action potential (AP) firing. When indicated, i.e. in DRG neurons isolated from CCI mice, the current injected was halved to 15 pA to avoid AP saturation. Action potential firing was quantified by counting the number of APs evoked by the ramp current. The $A_3\text{AR}$ agonist was applied by superfusion, and its effect on AP number was evaluated after at least 5 min of extracellular flow interruption and at the end of a 8 min application. When applied in the presence of the anti-IL-10 antibody (R&D System; $0.5 \mu\text{g}/\text{ml}$), the $A_3\text{AR}$ agonist was added at least 10 min after the Ab. When indicated, IL-10 (Sigma-Aldrich, 10-500 ng/ml) was applied by superfusion.

Statistical analysis

Data are expressed as means \pm SD for n animals. No differences were observed between male and female mice behaviour ($p < 0.05$) and therefore, where indicated, data were expressed as a single group. Behavioural data were analysed by one-way, two-way, or repeated measures ANOVA with post hoc t-tests, Tukey, Sidak or Dunnett's pair-wise comparisons to control. Significant differences were defined as a value of $p < 0.05$. Electrophysiology and immunofluorescence averaged data are reported as mean \pm SEM for n cells or animals tested. Student's paired t -test was used for statistical comparisons between data obtained from the same cell before and after treatment or between ipsilateral and contralateral DRGs. Significant differences were defined as a value of $p < 0.05$. All statistical analysis was performed using GraphPad Prism 8.4 (GraphPad Software, San Diego CA USA).

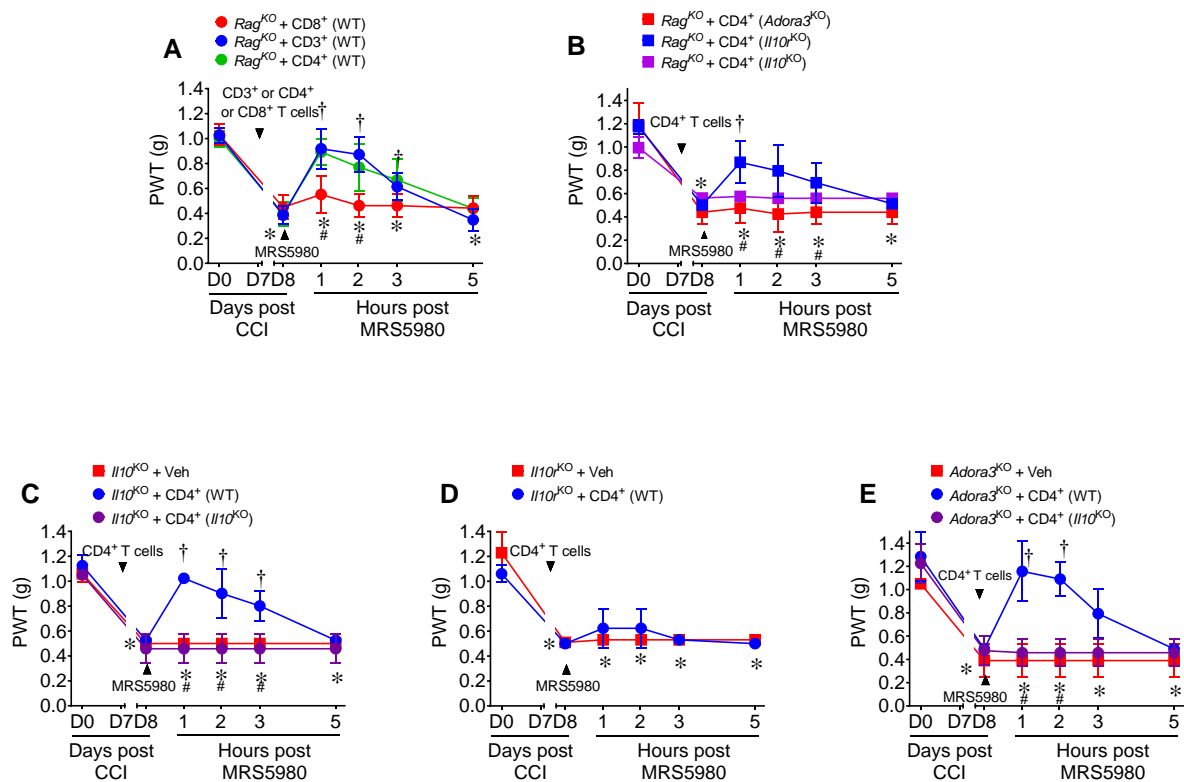


Figure S1. Timecourse of A₃AR agonist effect in *Rag*^{KO}, *Il10*^{KO}, *Il10r*^{KO} and *Adora3*^{KO} mice. Adoptive transfer of CD3⁺ (n=5) or CD4⁺ (n=20 males and females) T cells but not CD8⁺-T (n=9) from WT mice into *Rag*^{KO} mice restored the anti-allodynic effects of MRS5980 (1 mg/kg, i.p.) lost in *Rag*^{KO} mice (A). Adoptive transfer of CD4⁺-T from *Adora3*^{KO} mice (B, n=4) failed to restore the anti-allodynic effect of MRS5980. The anti-allodynic effect of MRS5980 lost in both male and female *Rag*^{KO} after adoptive transfer of CD4⁺-T from *Il10*^{KO} mice (n=11) was restored after adoptive transfer of CD4⁺-T from *Il10r*^{KO} mice (n=9) (B). The anti-allodynic effect of MRS5980 were lost in *Il10*^{KO} (C, n=6) and *Il10r*^{KO} (D, n=6) mice. Adoptive transfer of CD4⁺-T from WT (n=6) but not from *Il10*^{KO} (n=6) mice restored the anti-allodynic effects of MRS5980 in *Il10*^{KO} mice (C). Conversely, adoptive transfer of CD4⁺-T from WT (D, n=6) mice did not restore the anti-allodynic effects of MRS5980 in *Il10r*^{KO} mice. The anti-allodynic effect of MRS5980 were lost in *Adora3*^{KO} mice (E, n=4). Adoptive transfer of CD4⁺-T from WT (n=6) but not from *Il10*^{KO} (n=4) mice restored the anti-allodynic effects of MRS5980 in *Adora3*^{KO} mice (E). Data are mean ± SD for n mice; *, p < 0.05 vs D0; †, p < 0.05 vs D8 by two-way repeated measures ANOVA with Dunnett's pair-wise comparisons. ; #, p < 0.05 vs *Rag*^{KO}+CD3⁺/CD4⁺ (WT) (A) or *Rag*^{KO}+CD4⁺ (*Il10r*^{KO}) (B) or *Il10*^{KO}+CD4⁺ (WT) (C) or *Adora3*^{KO}+CD4⁺ (WT) (D) by two-way repeated measures ANOVA with Tukey's pair-wise comparisons.

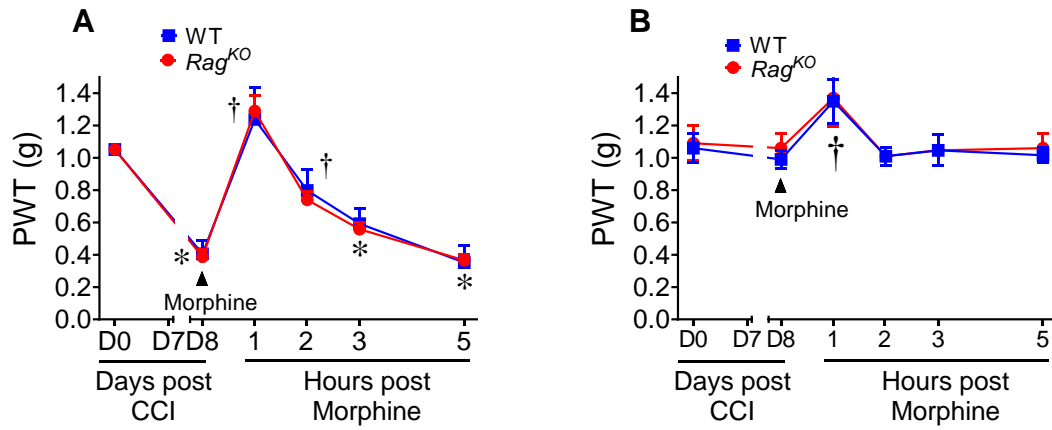


Figure S2. Anti-allodynic effects of morphine were not affected in *Rag*^{KO} mice. The analgesic effect of subcutaneous injection of morphine (3 mg/kg; n=5) was similar in CCI *Rag*^{KO} and WT mice (**A**, ipsilateral paw; **B**, contralateral paw). Data are expressed as mean \pm SD and analyzed by two-way ANOVA with Dunnett's comparisons. *, $p < 0.05$ vs D0; †, $p < 0.05$ vs. D8.

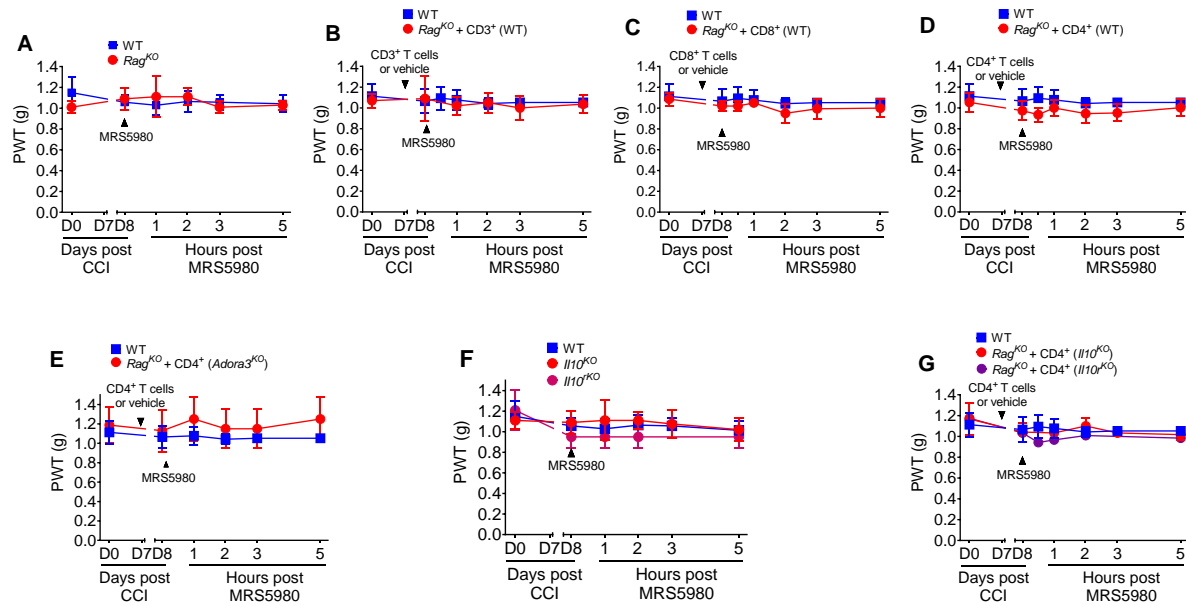


Figure S3. A₃AR agonists had no effects on contralateral paw pain behavior. A systemic (A, 1 mg/kg, i.p.; WT n=7, Rag^{KO} n=6; F, 1 mg/kg, i.p.; n=5/group) injection of MRS5980 on D8 after CCI in WT, Il10^{KO}, Il10^{rKO} and Rag^{KO} mice did not alter the contralateral paw pain baseline level as well as in Rag^{KO} (B n=5; C, n=9; D, n=15; E, n=4; G, n=6) CCI mice that were previously injected (D7, i.v.) with CD3⁺, CD4⁺ or CD8⁺ T from WT (B, C, D), Adora3^{KO} (E), Il10^{KO} or Il10^{rKO} (G) mice. Data are expressed as mean ± SD for n mice.

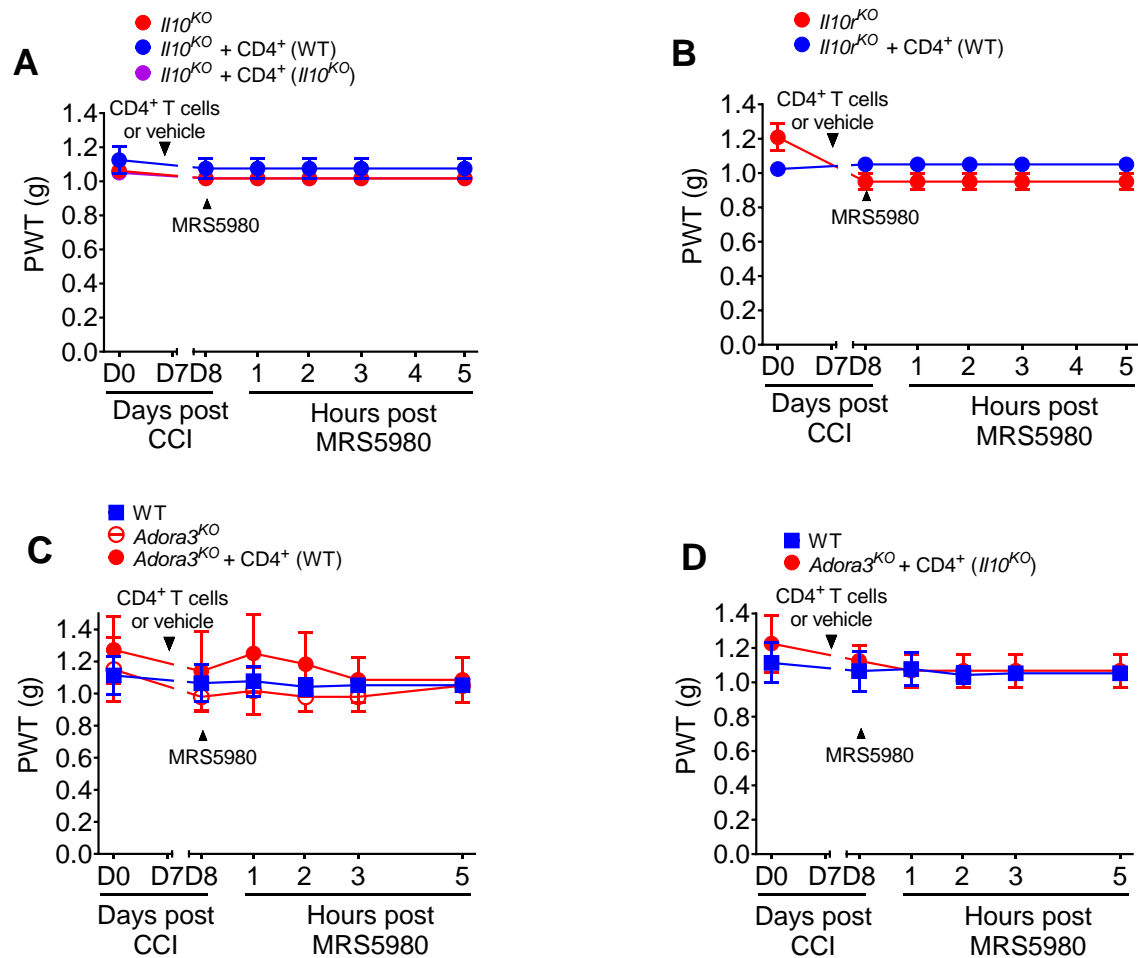


Figure S4. A₃AR agonists had no effects on contralateral paw pain behavior. A systemic (A-D, 1 mg/kg, i.p.; n=6/group) injection of MRS5980 on D8 after CCI in WT, *Il10*^{KO}, *Il10r*^{KO} and *Adora3*^{KO} mice did not alter the contralateral paw pain baseline level as well as in *Il10*^{KO} (A, n=6/group), *Il10r*^{KO} (B, n=6/group) and *Adora3*^{KO} (C, n=9; D, n=4) CCI mice that were previously injected (D7, i.v.) with CD4⁺-T from WT (A, B, C) or *Il10*^{KO} (A,D) mice. Data are expressed as mean ± SD for n mice.

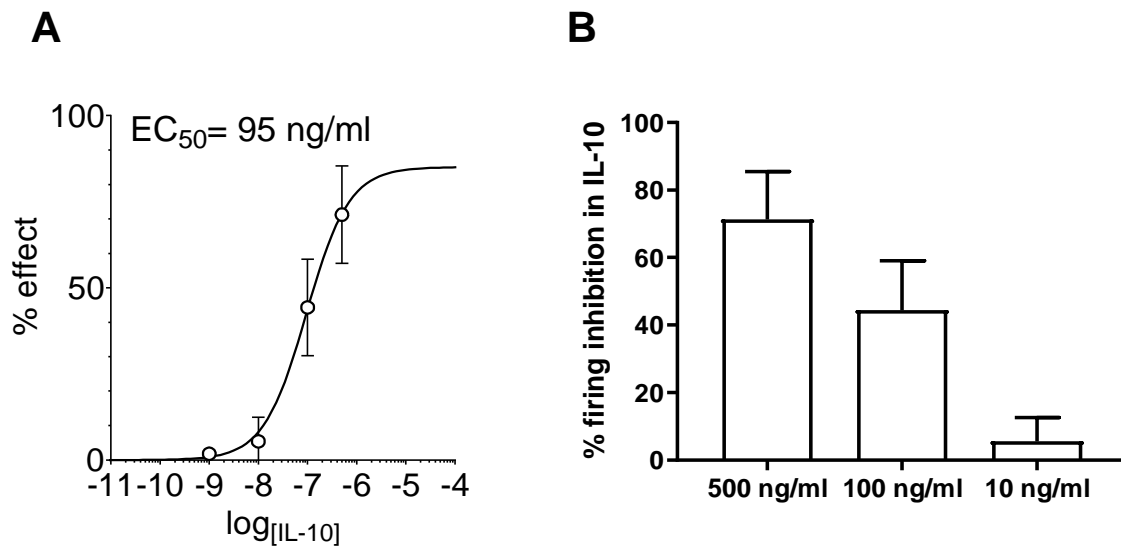


Figure S5. Concentration-response curve and EC₅₀ of IL-10 on AP firing in mouse DRG neurons. The EC₅₀ for IL-10 on DRG firing was 95 ng/ml (**A**) and approximately 70% inhibition was obtained with 500 ng/ml (**B**).

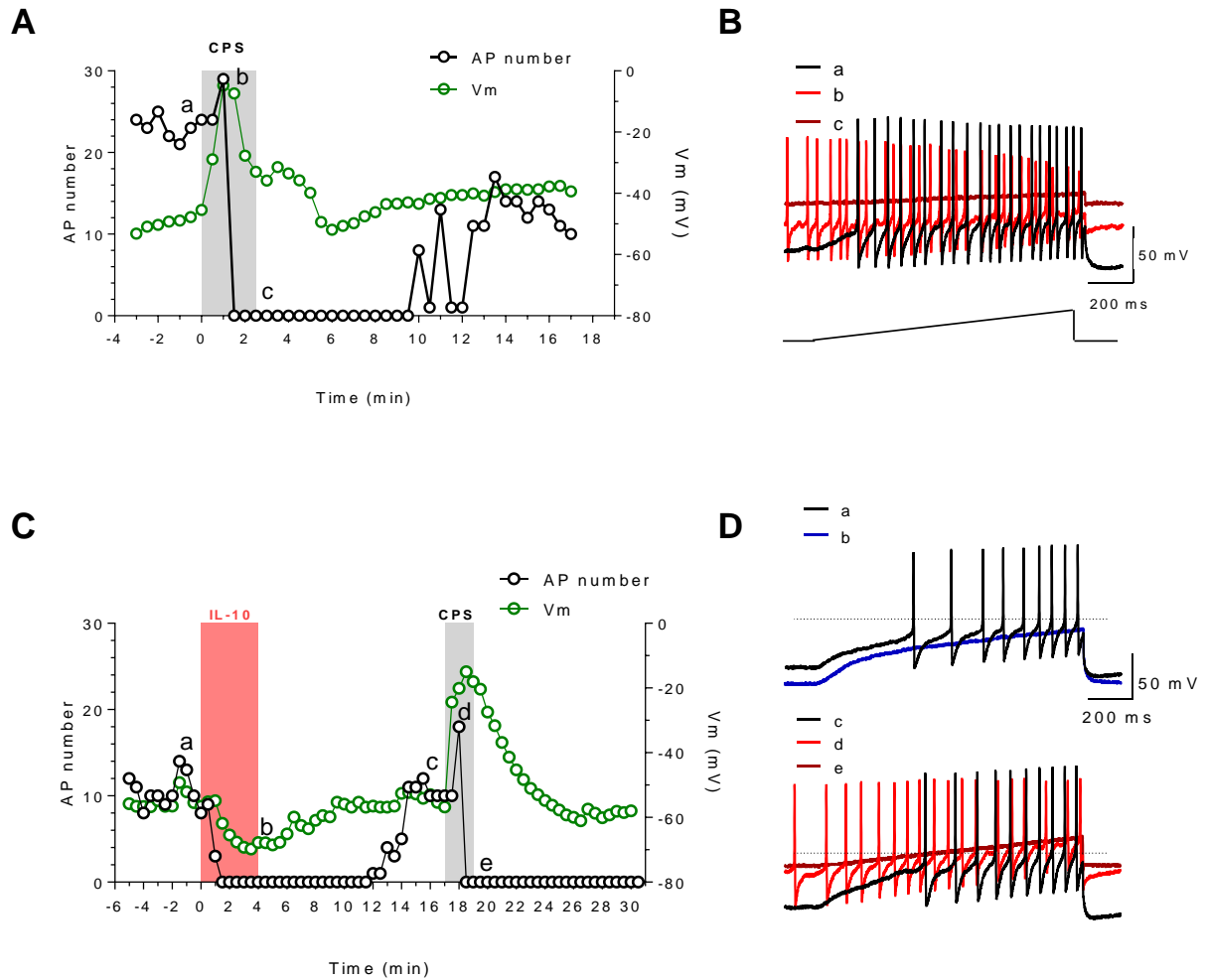


Figure S6. Effects of IL-10 and/or capsaicin application on DRG neurons isolated from naïve mice. The effects of the transient receptor potential vanilloid 1 (TRPV1) agonist capsaicin (CPS, 1 μ M) alone (**A**) or after IL-10 (100 ng/ml) application (**C**) on resting membrane potential (Vm: open green circles) or action potential (AP) firing (open black circles) were pooled as a function of time in two representative DRG neurons isolated from naïve mice. Similar results were obtained in $n=3$ cells for CPS application, and $n=6$ cells for CPS superfusion after IL-10. Original voltage traces recorded in respective cells at representative time points (**B,D**). AP firing was evoked by a 1 s, 30 pA ramp current injection (lower inset in B).

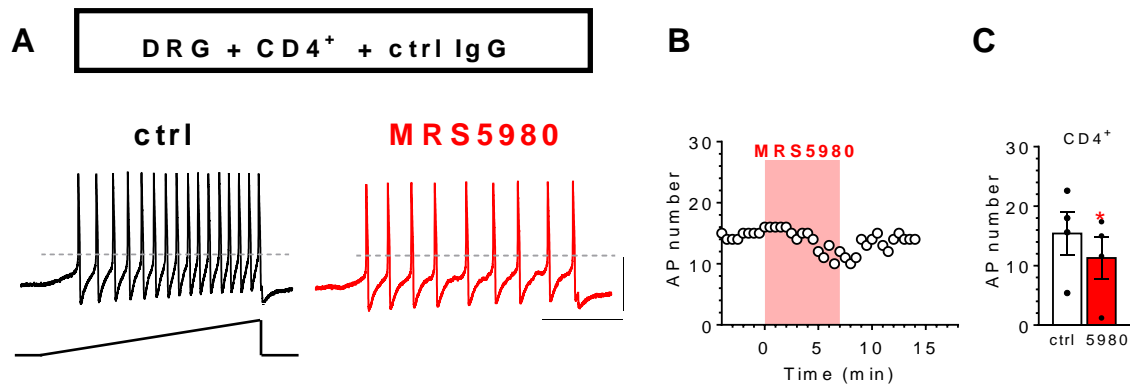


Figure S7. The effect of MRS5980 on DRG neuron cell firing in the presence of CD4⁺-T is not affected by control IgG isotype. Original current-clamp traces recorded by whole-cell patch-clamp technique in a typical naïve mouse DRG neuron co-cultured with naïve CD4⁺-T where the A₃AR agonist MRS5980 (300 nM) inhibits action potential (AP) firing when applied in the presence of a control IgG isotype (ctrl IgG) (**A**). AP firing was evoked by a depolarizing ramp current injection (1 s; 30 pA: lower inset in A) once every 30 s. Dotted grey lines indicate the 0 mV level. The number of APs elicited by the current ramp was plotted as a function of time in the same cell (**B**) or was expressed as pooled data (mean ± SEM) in the bar graph (**C**, n=4). *, p = 0.0028, paired Student's *t*-test; Scale bars: 300 ms; 50 mV.

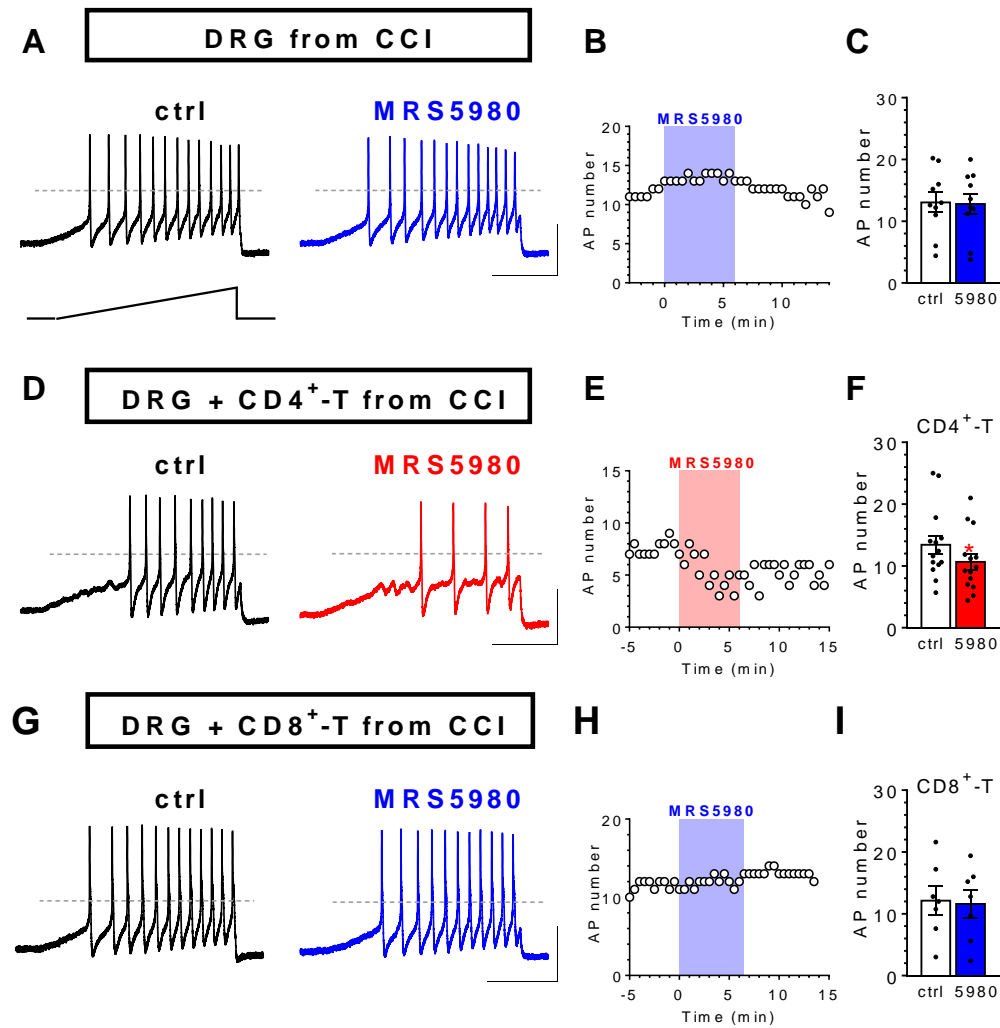


Figure S8. MRS5980 decreases action potential firing in DRG neurons-CD4⁺-T co-cultures isolated from mice after chronic constriction injury. **A,D,G.** Original current-clamp traces recorded by whole-cell patch-clamp technique in typical mouse DRG neurons isolated from C57BL/6 mice 7 days after chronic constriction injury (CCI). Action potential (AP) firing was evoked by a depolarizing ramp current injection (1 s; 15 pA; lower inset) once every 30 s. The A₃AR agonist MRS5980 (300 nM) was applied in DRG cultures (**A**), in DRG neurons co-cultured with CD4⁺ (**D**) or CD8⁺-T (**G**) isolated from CCI animals. The number of APs elicited by the current ramp was plotted as a function of time in four different representative cells (**B,E,H**) or was expressed as pooled data (mean ± SEM) in the bar graphs (**C**, n=10; **F**, n=14; **I**, n=7). Dotted grey lines indicate the 0 mV level. *, p = 0.0177, paired Student's *t*-test. Scale bars: 300 ms; 50 mV.

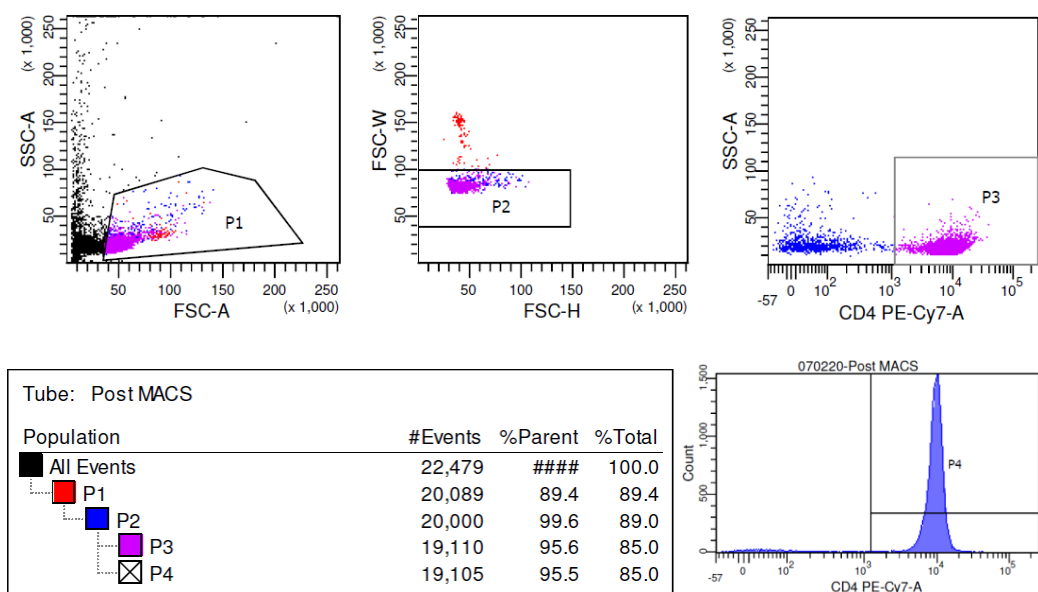


Figure S9. T cells purity assessment by flow cytometry. A representative flow cytometry analysis from WT mice showed more than 95% of CD4⁺ T cells.

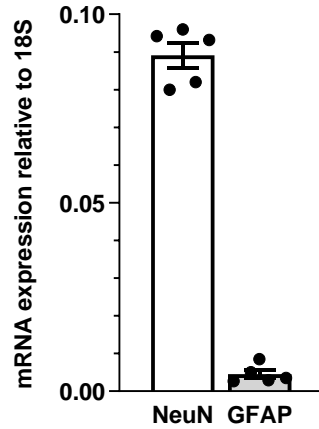


Figure S10. DRG cell cultures are predominantly neuronal. RT-qPCR analysis showed high mRNA levels of the neuronal marker NeuN in comparison to GFAP as satellite cells marker. 18S was used as housekeeping gene. Data are mean \pm SEM of 5 biological samples.

	Cell diameter (μm)		V _m (mV)	Current threshold (pA)
DRG	18.2 ± 2.2	ctrl	-58.0 ± 3.9	4.4 ± 0.2
		MRS5980	-56.6 ± 6.0	3.5 ± 1.2
DRG from CCI		ctrl	-55.2 ± 1.4	2.4 ± 0.3 [@]
		MRS5980	-53.4 ± 1.3	2.0 ± 0.3
DRG + CD4 ⁺ -T	20.3 ± 1.7	ctrl	-59.6 ± 2.9	4.7 ± 0.7
		MRS5980	-57.9 ± 3.3	10.4 ± 1.1 [*]
DRG + CD4 ⁺ -T from CCI		ctrl	-53.3 ± 1.7	1.9 ± 0.3 ^{@@}
		MRS5980	-53.4 ± 2.0	2.7 ± 0.5 [^]
DRG + CD4 ⁺ -T + Ab IL-10	18.0 ± 1.2	ctrl	-55.6 ± 2.6	7.3 ± 0.1
		MRS5980	-53.6 ± 3.4	6.7 ± 0.1
DRG + CD8 ⁺ -T	18.3 ± 1.3	ctrl	-53.0 ± 3.5	4.5 ± 0.9
		MRS5980	-52.7 ± 2.9	4.1 ± 0.8
DRG + CD8 ⁺ -T from CCI	15.8 ± 3.5	ctrl	-51.3 ± 3.6	2.2 ± 0.7 ⁺⁺
		MRS5980	-50.4 ± 4.2	2.2 ± 0.9
DRG + IL-10	19.8 ± 3.2	ctrl	-55.1 ± 4.6	5.3 ± 2.9
		IL-10	-57.2 ± 7.3	10.9 ± 4.4 [#]

Table S1. Current-clamp parameters measured in mouse DRG neurons in the whole-cell mode

The following experimental groups were analyzed: DRG neurons (DRG, n=6); DRG neurons isolated 7 days after chronic constriction injury (CCI) (DRG from CCI, n=10); DRG + CD4⁺-T (DRG + CD4⁺-T, n=10); DRG + CD4⁺-T, both cell types isolated from CCI mice (DRG + CD4⁺-T from CCI, n=14); DRG neurons + CD4⁺-T in the presence of anti-IL-10-antibody (0.5 μg/ml) (DRG + CD4⁺-T + Ab IL-11); DRG neurons + CD8⁺-T (DRG + CD8⁺-T, n=7); DRG neurons + CD8⁺-T isolated from CCI mice (DRG + CD8⁺-T from CCI, n=7); DRG neurons + IL-10 application (0.5 μg/ml) (DRG + IL-10; n=6). Cell diameter was calculated from cell capacitance of an approximated spherical cell shape accordingly to the equation of the sphere surface: $A=4\pi r^2$ (16). Resting membrane potential (V_m) was measured as the averaged membrane voltage during the 100 ms preceding each current ramp and was corrected for the calculated liquid junction potential (14.1 mV); AP parameters are referred to the first AP generated by the current ramp. The current needed to produce the first spike was defined as “current threshold” and was measured (in pA) as the minimal amount of current injected during the ramp protocol which achieved AP initiation. *, p = 0.0316; ^, p = 0.0413; #, p = 0.0412 vs respective ctrl, paired Student's *t*-test. @, p = 0.0105 vs respective value in DRG; @@ p = 0.0038 vs respective value in DRG + CD4⁺-T; ++, p = 0.0385 vs respective value in DRG + CD8⁺-T, unpaired Student's *t*-test. Data are mean ± SEM.

References

1. Salvatore CA, Tilley SL, Latour AM, Fletcher DS, Koller BH, and Jacobson MA. Disruption of the A(3) adenosine receptor gene in mice and its effect on stimulated inflammatory cells. *The Journal of biological chemistry*. 2000;275(6):4429-34.
2. Tosh DK, Deflorian F, Phan K, Gao ZG, Wan TC, Gizewski E, et al. Structure-guided design of A(3) adenosine receptor-selective nucleosides: combination of 2-arylethynyl and bicyclo[3.1.0]hexane substitutions. *J Med Chem*. 2012;55(10):4847-60.
3. Tosh DK, Padia J, Salvemini D, and Jacobson KA. Efficient, large-scale synthesis and preclinical studies of MRS5698, a highly selective A3 adenosine receptor agonist that protects against chronic neuropathic pain. *Purinergic Signal*. 2015;11(3):371-87.
4. Little JW, Ford A, Symons-Liguori AM, Chen Z, Janes K, Doyle T, et al. Endogenous adenosine A3 receptor activation selectively alleviates persistent pain states. *Brain*. 2015;138(Pt 1):28-35.
5. Tosh DK, Finley A, Paoletta S, Moss SM, Gao ZG, Gizewski ET, et al. In vivo phenotypic screening for treating chronic neuropathic pain: modification of C2-arylethynyl group of conformationally constrained A3 adenosine receptor agonists. *J Med Chem*. 2014;57(23):9901-14.
6. Byers SL, Wiles MV, Dunn SL, and Taft RA. Mouse estrous cycle identification tool and images. *PLoS One*. 2012;7(4):e35538.
7. Chen Z, Doyle TM, Luongo L, Largent-Milnes TM, Giancotti LA, Kolar G, et al. Sphingosine-1-phosphate receptor 1 activation in astrocytes contributes to neuropathic pain. *Proc Natl Acad Sci U S A*. 2019.
8. Dixon WJ. Efficient analysis of experimental observations. *Annual review of pharmacology and toxicology*. 1980;20:441-62.
9. Janes K, Little JW, Li C, Bryant L, Chen C, Chen Z, et al. The development and maintenance of paclitaxel-induced neuropathic pain require activation of the sphingosine 1-phosphate receptor subtype 1. *The Journal of biological chemistry*. 2014;289(30):21082-97.
10. Chaplan SR, Bach FW, Pogrel JW, Chung JM, and Yaksh TL. Quantitative assessment of tactile allodynia in the rat paw. *J Neurosci Methods*. 1994;53(1):55-63.
11. Richner M, Jager SB, Siupka P, and Vaegter CB. Hydraulic Extrusion of the Spinal Cord and Isolation of Dorsal Root Ganglia in Rodents. *J Vis Exp*. 2017(119).
12. Schindelin J, Arganda-Carreras I, Frise E, Kaynig V, Longair M, Pietzsch T, et al. Fiji: an open-source platform for biological-image analysis. *Nat Methods*. 2012;9(7):676-82.
13. Haase R, Royer LA, Steinbach P, Schmidt D, Dibrov A, Schmidt U, et al. CLIJ: GPU-accelerated image processing for everyone. *Nat Methods*. 2020;17(1):5-6.
14. Coppi E, Cherchi F, Fusco I, Failli P, Vona A, Dettori I, et al. Adenosine A3 receptor activation inhibits pronociceptive N-type Ca²⁺ currents and cell excitability in dorsal root ganglion neurons. *Pain*. 2019;160(5):1103-18.
15. Coppi E, Pedata F, and Gibb AJ. P2Y(1) receptor modulation of Ca²⁺-activated K⁺ currents in medium-sized neurons from neonatal rat striatal slices. *Journal of Neurophysiology*. 2012;107(3):1009-21.
16. Hille B. *Ion channels of excitable membranes*. Sunderland, Mass.: Sinauer; 2001.